to facilitate their extravasation and metastasis. Keratan, heparan, chondroitin, carbohydrate, and tyrosine sulfate have been detected on alternatively spliced, higher molecular weight forms (116 to 200 kD) of CD44 (*16, 17*). In our study, the 85-kD form of CD44 was the major sulfated moiety. Preliminary data from sulfo–amino acid analysis provided no evidence for the tyrosine sulfation of CD44, whereas chemical or enzymatic removal of carbohydrate did provide evidence for carbohydrate sulfation (*18*). However, the precise identification of the sulfated residues and their location within CD44 remain to be determined. The selectin ligands are cell adhesion molecules involved in leukocyte–endothelial cell interactions that are also sulfated (*19*). These molecules mediate the initial rolling interactions between leukocytes and high-walled endothelial venules (HEVs) (*20*). Sulfation of two selectin ligands, GlyCAM-1 and CD34, occurs in HEVs on O-linked glycans and is required for high-affinity binding to L-selectin (*19, 21*). Tyrosine sulfation of the P-selectin ligand PSGL-1, present on leukocytes, has been shown to be important for high-affinity binding to P-selectin (*22*). Thus, the sulfation of cell adhesion molecules on HEVs and leukocytes may occur to facilitate leukocyte–endothelial cell interactions. The induction of CD44 sulfation by TNF-α provides one potential mechanism for regulating leukocyte adhesion during an inflammatory response.

References and Notes

1. T. A. Springer, *Cell* **76**, 301 (1994); E. C. Butcher and L. J. Picker, *Science* **272**, 60 (1996).
2. R. L. Camp, A. Scheynius, C. Johansson, E. Puré, *J. Exp. Med.* **178**, 497 (1993); H. C. DeGrendele, P. Estess, L. J. Picker, M. H. Siegelman, *ibid.* **183**, 1119 (1996); R. A. Clark, R. Alon, T. A. Springer, *J. Cell Biol.* **134**, 1075 (1996); H. C. DeGrendele, P. Estess, M. H. Siegelman, *Science* **278**, 672 (1997).
3. J. Lesley, R. Hyman, P. W. Kincade, *Adv. Immunol.* **54**, 271 (1993).
4. J. Lesley, R. Hyman, N. English, J. B. Catterall, G. A. Turner, *Glycoconj. J.* **14**, 611 (1997).
5. P. W. Kincade, Z. Zheng, S. Katoh, L. Hanson, *Curr. Opin. Cell Biol.* **9**, 635 (1997).
6. M. P. Bevilacqua, *Annu. Rev. Immunol.* **11**, 767 (1993).
7. M. C. Levesque and B. F. Haynes, *J. Immunol.* **159**, 6184 (1997).
8. H. G. Klingemann *et al.*, *Leuk. Lymphoma* **12**, 463 (1994).
9. SR91 cells (10^6 cells/ml) were stimulated with TNF-α (10 ng/ml) or IFN-γ (500 U/ml; R&D Systems) in RPMI medium with 10% fetal calf serum (FCS) for 24 hours at 37°C in the presence of 5% CO_2. Sodium chlorate (50 mM; Sigma) was added concurrent with the cytokine treatment. Labeling of cells with mAbs or FL-hyaluronan for flow cytometry was as described (*14*). Cells were analyzed on a FACScan flow cytometer (Becton Dickinson) using Lysis II software.
10. Unstimulated and stimulated SR91 cells (10^6 cells/ml) were resuspended in 25 μM CellTracker Green 5-chloromethylfluorescein diacetate (CMFDA; Molecular Probes) in RPMI medium for 30 min at 37°C, resuspended in RPMI with 10% FCS for 30 min at 37°C, and then washed. SR91 cells (3×10^5) were incubated with a confluent monolayer of SVEC4-10 cells in 0.5 ml of phosphate-buffered saline (PBS) with 2% FCS (in a 24-well plate) for 30 min at room temperature, then washed four times with PBS. Cells were fixed in 4% paraformaldehyde and analyzed on a Cytofluor 2300 fluorimeter (Millipore) or photographed (Zeiss Axiophot). For inhibition studies, cells were pretreated with purified CD44 mAb IM7.8.1 [I. S. Trowbridge, J. Lesley, R. Schulte, R. Hyman, J. Trotter, *Immunogenetics* **15**, 299 (1982)], CD44 mAb KM201 [K. Miyake *et al.*, *J. Exp. Med.* **171**, 477 (1990)], or ICAM-1 mAb (Cedarlane) in PBS (3 μg/ml) with 2% FCS, rooster comb hyaluronan (50 μg/ml; Sigma), or ovine hyaluronidase (5 μg/ml; Calbiochem) and incubated for 20 min at 4°C after the labeling period. Cells were washed twice before mixing. CMFDA-labeled SR91 cells (3×10^5; 100% input cells) and wells containing the monolayer alone were used to determine 100% binding and background levels, respectively.
11. K. A. O'Connell and M. Edidin, *J. Immunol.* **144**, 521 (1990).
12. A. Maiti and P. Johnson, unpublished data.
13. P. A. Baeuerle and W. B. Huttner, *Biochem. Biophys. Res. Commun.* **141**, 870 (1986).
14. L. E. Esford, A. Maiti, S. A. Bader, F. Tufaro, P. Johnson, *J. Cell Sci.* **111**, 1021 (1998).
15. Cells (10^6 cells/ml) were labeled with 100 μCi/ml of [^{35}S]sulfate (~43 Ci/mg; ICN) in RPMI medium with 2% FCS for 24 hours at 37°C in the presence of 5% CO_2. For each sample, 5×10^6 cells were labeled and samples treated with cytokine or chlorate, as described above. Cells were then lysed, precleared, CD44-immunoprecipitated, electrophoresed, and autoradiographed or immunoblotted as described (*14*).
16. S. Jalkanen, M. Jalkanen, R. Bargatze, M. Tammi, E. C. Butcher, *J. Immunol.* **141**, 1615 (1988).
17. T. A. Brown, T. Bouchard, T. St. John, E. Wayner, W. G. Carter, *J. Cell Biol.* **113**, 207 (1991); K. Takahashi, I. Stamenkovic, M. Cutler, A. Dasgupta, K. K. Tanabe, *J. Biol. Chem.* **271**, 9490 (1996); J. P. Sleeman, U. Rahmsdorf, A. Steffen, H. Ponta, P. Herrlich, *Eur. J. Biochem.* **255**, 74 (1998).
18. A. Maiti and P. Johnson, unpublished data.
19. S. D. Rosen and C. R. Bertozzi, *Curr. Biol.* **6**, 261 (1996).
20. A. Varki, *Proc. Natl. Acad. Sci. U.S.A.* **91**, 7390 (1994); J. P. Girard and T. A. Springer, *Immunol. Today* **16**, 449 (1995).
21. Y. Imai, L. A. Lasky, S. D. Rosen, *Nature* **361**, 555 (1993); S. Hemmerich, E. C. Butcher, S. D. Rosen, *J. Exp. Med.* **180**, 2219 (1994).
22. D. Sako *et al.*, *Cell* **83**, 323 (1995); T. Pouyani and B. Seed, *ibid.*, p. 333.

23. Supported by research grants from the National Science and Engineering Research Council and the Arthritis Society of Canada. A.M. was supported by a studentship from the Heart and Stroke Foundation of British Columbia and Yukon. We thank H. Klingemann for providing the SR91 cell line.

28 July 1998; accepted 2 October 1998

Extended Life-Span and Stress Resistance in the *Drosophila* Mutant *methuselah*

Yi-Jyun Lin, Laurent Seroude, Seymour Benzer*

Toward a genetic dissection of the processes involved in aging, a screen for gene mutations that extend life-span in *Drosophila melanogaster* was performed. The mutant line *methuselah* (*mth*) displayed approximately 35 percent increase in average life-span and enhanced resistance to various forms of stress, including starvation, high temperature, and dietary paraquat, a free-radical generator. The *mth* gene predicted a protein with homology to several guanosine triphosphate–binding protein–coupled seven–transmembrane domain receptors. Thus, the organism may use signal transduction pathways to modulate stress response and life-span.

The effect of genes on life-span in *Drosophila* has been established by selective breeding (*1*). However, the participation of multiple genes with additive, quantitative effects can be difficult to unravel. A direct search for life-extension mutants could identify individual genes that regulate biological aging. Indeed, in the nematode *Caenorhabditis elegans*, several mutations, for example, *age-1*, *daf-2*, and *clk-1*, have been described that can increase the worm's life-span (*2*). The corresponding genes have been cloned and are involved in various aspects of development and metabolism (*3*, *4*).

Life-span and stress response are closely associated. In *C. elegans*, the *age-1* mutant displays elevated resistance to thermal exposure (*5*) and to oxidative stress (*6*). In *Drosophila*, laboratory stocks selected for postponed senescence also show increased tolerance to heat, starvation, desiccation, and oxidative damage (*7–9*). Tandem overexpression of Cu-Zn superoxide dismutase (SOD) and catalase genes in *Drosophila* increased life-span by 30% (*10*). Similar observations were made in flies expressing the human SOD1 transgene in motor neurons (*11*). However, the physiological and molecular events involved in life-span determination and stress resistance have remained largely elusive.

We generated a set of P-element insertion lines (*12*, *13*) and screened them for ones that outlived a parent strain (*white*^{1118}). *methuselah* (*mth*) was isolated by its increase in life-span at 29°C. The life extension was confirmed at 25°C. At both temperatures, flies homozygous for the P-element lived, on the average, 35% longer than the parent strain (Fig. 1).

We then examined the ability of *mth* flies to resist stress. *mth* mutant flies were more resis-

Division of Biology, California Institute of Technology, Pasadena, CA 91125, USA.

*To whom correspondence should be addressed. E-mail: benzer@caltech.edu

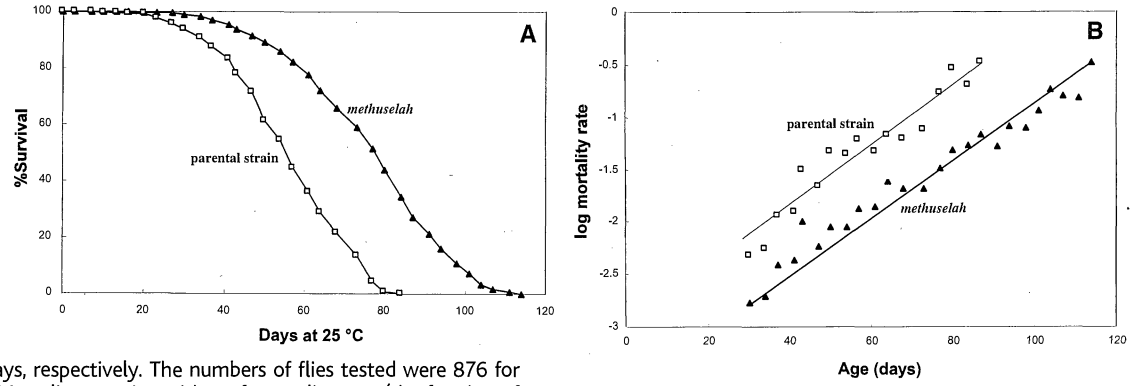

Fig. 1. Life-span extension in *methuselah*. Male flies of the parental strain (*white*^{1118}) and *methuselah* (homozygous for the P-element insertion) were maintained in a constant temperature, humidity, and 12/12 hour dark/light cycle environment. Flies were transferred to fresh food vials and scored for survival every 3 to 4 days. (**A**) Survival curve. The average life-spans for w^{1118} and *mth* were 57 and 77 days, respectively. The numbers of flies tested were 876 for w^{1118} and 783 for *mth*. (**B**) Mortality rate. Logarithm of mortality rate (the fraction of flies dying per day) is plotted against age.

tant to dietary paraquat (Fig. 2A), which, upon intake by the cell, generates superoxide anion (*14*). At a concentration of 20 mM, paraquat rendered normal males sluggish by 12 hours; at 48 hours, nearly 90% were dead. In contrast, *mth* males were still active at 24 hours, and at 48 hours more than 50% were still alive. In a long-lived strain of *Drosophila* derived by selection, life-span extension also accompanies increased paraquat resistance (*9*). Transgenic *Drosophila* carrying extra copies of SOD and catalase, two primary components of the defense system against reactive oxygen species, also have increased life-span (*10*). Flies transgenic for the human SOD1 gene display increased life-span and paraquat resistance, the degree of effect correlating with dosage of the transgene (*11*). Thus, *mth* may have a higher capacity of the free-radical defense system.

In the starvation test, *mth* showed a greater than 50% increase in average survival time over the parent strain (Fig. 2B). Females were consistently more resistant than males, suggesting that their larger body weight may contribute to resistance. Indeed, *mth* males and females weighed 20 to 30% more than their w^{1118} counterparts. In a *Drosophila* stock selectively bred for postponed senescence, resistance to starvation and lipid content are higher than the baseline stock (*7*). In *C. elegans*, the mutant *daf-2*, which exhibits marked increase in longevity, has extensive fat accumulation when grown at 25°C, suggesting a coupling of its metabolism with longevity (*4*).

Next we tested exposure to high temperature (Fig. 2C). At 36°C, *mth* survived longer than the parent strain. Heat shock proteins, a class of molecular chaperones, are thought to counter stress-induced detrimental effects during aging (*15*). In a transgenic fly harboring 12 additional copies of the heat-inducible *hsp70* gene, there was a positive correlation between life expectancy and elevated Hsp70 protein expression (*16*). Correspondingly, in *daf-2* and *age-1* mutant worms, resistance to thermal stress was higher than in control animals (*5*). The increased thermotolerance of *mth* may result from higher expression of heat shock proteins and related molecular chaperones.

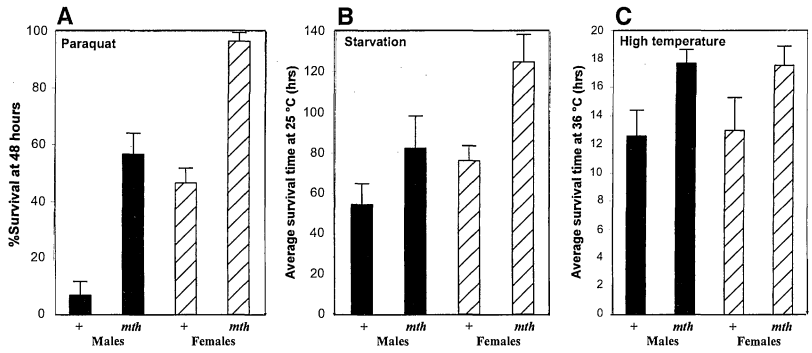

Fig. 2. Stress responses. Homozygous *mth* compared with the parent strain. Newly eclosed flies were sex-segregated, distributed 20 per vial, and maintained in fresh food vials for 2 to 5 days before testing. Genotypes and sexes are indicated. (**A**) Paraquat resistance. Flies (age 2 days) were starved for 6 hours, then transferred to vials (2.5 cm by 9.3 cm) containing two 2.4-cm glass-fiber filter circles (Whatman) wetted with 20 mM paraquat (Sigma) in 5% sucrose solution, and survival was scored at 25°C. The ingestion rates of *mth* and the parent strain were similar, as determined by ^{14}C-leucine and dye intake. (**B**) Starvation test. Flies (age 2 days) were transferred to vials containing filters moisturized with 0.2 ml of distilled water. Distilled water was added to keep the filters moist during the test. (**C**) Thermal stress test. Flies (age 5 days) were transferred to vials containing 1% agar in 5% sucrose solution, and maintained at 36°C.

By Southern (DNA) blot analysis of *mth* genomic DNA, we confirmed that *mth* carries a single P-element insertion in the genome (*17*). Genetic mapping indicated that it is inserted in the third chromosome. By crossing *mth* to flies harboring a transposase (*18*), we generated lines in which the P-element was precisely excised from the insertion site (as determined by polymerase chain reaction). Eight lines obtained in this manner had life-spans reverted to that of the parent strain, indicating that the phenotype in *mth* was specifically caused by the P-element insertion. The precise-excision strains were used as controls throughout the study; they behaved similarly to the parental strain in stress resistance as well.

Two other lines isolated had imprecise excisions of the P-element, resulting in deletion of DNA adjacent to the insertion site. Both of these lines, which likely represent null alleles of the *mth* gene, displayed pre-adult lethality in homozygotes, suggesting that the gene also plays an essential role in development. Flies heterozygous for the P-element over an imprecise excision allele were more resistant to stress than those homozygous for the P-element, indicating that the mutation created by the P-element insertion is a hypomorphic allele. The P-element insertion in the third intron of the *mth* gene may reduce the level of gene expression by interfering with RNA splicing, without eliminating the gene function.

We cloned the full-length genomic and complementary DNA of the *mth* gene (*19*) (Fig. 3). The cDNA encodes a single open reading frame (Fig. 3B). The predicted protein sequence has a leader peptide plus seven hydrophobic regions suggestive of transmembrane (TM) domains (Fig. 3C). A gapped Blast search (*20*) of this sequence showed homology to a variety of guanosine triphosphate–binding regulatory protein (G protein)–coupled receptors (GPCRs) (Fig. 3D). GPCR was also predicted by the Blocks Search program (*21*). The amino acid residues between TM5 and TM6, especially those near the transmembranes, are highly basic, a feature shared by many G protein–linked receptors, and in some cases these residues interact directly with G proteins (*22*). Ho-

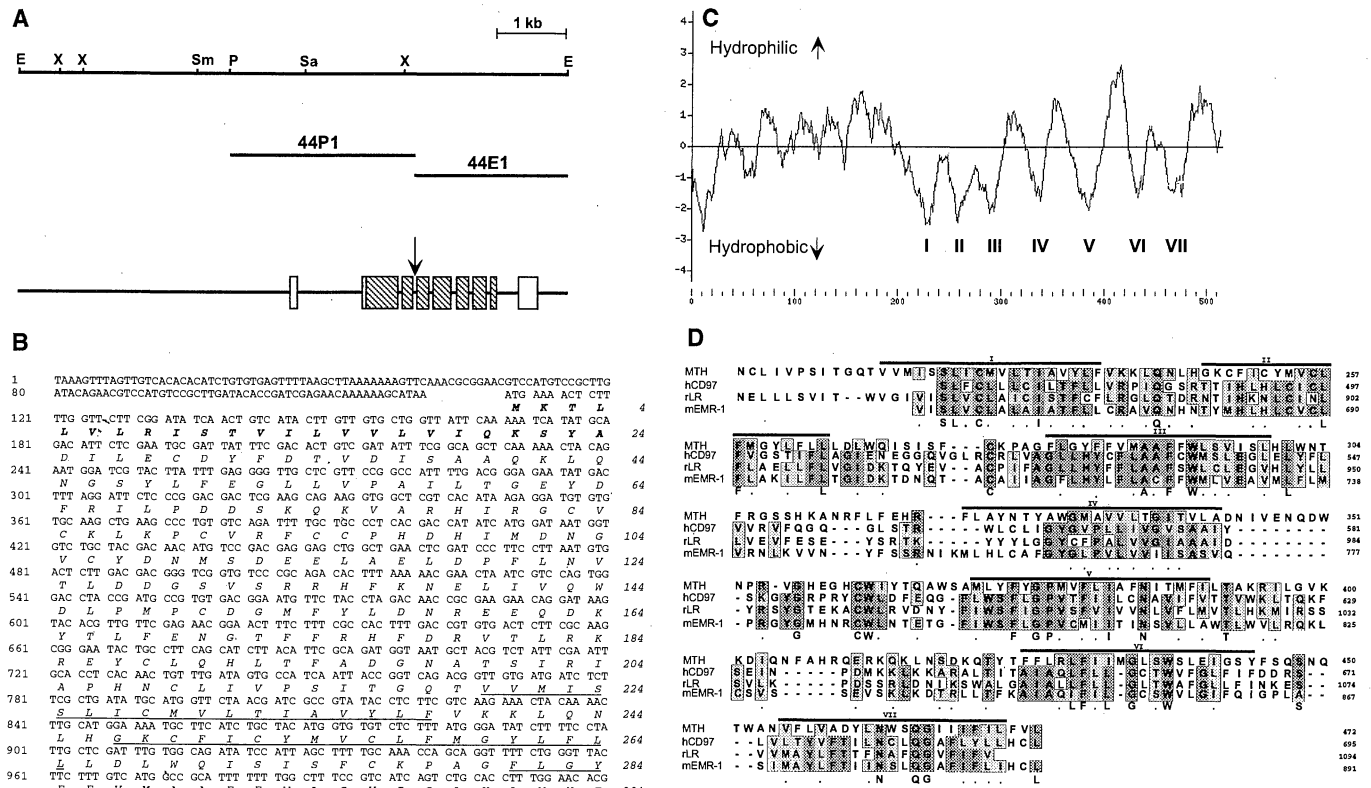

Fig. 3. The *mth* gene. The full-length cDNA and its corresponding genomic segment. (**A**) Genomic DNA. Restriction enzyme sites: E, Eco RI; P, Pst I; Sa, Sac I; Sm, Sma I; X, Xba I. Boxes indicate exons; hatched boxes, the open reading frame. The P-element insertion site is indicated by an arrow. The plasmid rescue clones, 44P1 and 44E1, represent, respectively, upstream and downstream fragments relative to the P-element. The structure is based on the genomic sequence derived from P1 plasmid DS06692 of the BDGP. (**B**) Complementary DNA and protein sequence. Numbers are indicated at the left and right, respectively. The putative leader peptide sequence is in boldface; TM domains are underlined. The polyadenylation site is boxed. The sequence is derived from LD08316 of the BDGP. (**C**) Hydropathic profile of the conceptual MTH protein, analyzed by the Kyte-Doolittle algorithm (*29*). The seven hydrophobic regions (excluding the NH_2-terminal, putative leader peptide) are designated. (**D**) Alignment of MTH with several known G protein–coupled receptors. MTH protein is aligned to partial sequences of human leukocyte surface antigen CD97 (hCD97, GenBank accession number P48960), rat α-latrotoxin receptor (rLR, U72487), and mouse epidermal growth factor module–containing receptor (mEMR-1, Q61549). Dark shading indicates identity, light shading similarity. The seven TM domains of MTH are indicated by lines above each row. Consensus amino acids are cited below; similarity is indicated by dots. Abbreviations for the amino acid residues are as follows: A, Ala; C, Cys; D, Asp; E, Glu; F, Phe; G, Gly; H, His; I, Ile; K, Lys; L, Leu; M, Met; N, Asn; P, Pro; Q, Gln; R, Arg; S, Ser; T, Thr; V, Val; W, Trp; and Y, Tyr.

mology was found mainly in the TM regions. The NH_2-terminal segment preceding the first TM domain was not found to share homology with any known sequence, thus diminishing the overall homology scores. The *mth* gene appears to represent a previously unknown member of the seven-TM protein superfamily. It remains to be seen whether the unique NH_2-terminal sequence is related to the regulation of the MTH protein, and what the identity of its ligand (or ligands) might be.

Because life-span and stress response are closely related, genetic screening by stress resistance provides an effective alternative to the much slower direct screening for lifetime (*23*). The ability of the *mth* fly to resist various kinds of stress is notable because there are likely to exist differences in pathways of response to individual forms of stress.

G protein–coupled receptors are involved in a remarkably diverse array of biological activities including neurotransmission, hormone physiology, drug response, and transduction of stimuli such as light and odorants (*24*). Our data suggest that MTH is a GPCR involved in stress response and biological aging. By regulating an associated G protein and thus its downstream pathway, the normal *mth* gene may maintain homeostasis and metabolism, playing a central role in modulating molecular events in response to stress. The pre-adult lethality of the null alleles demonstrates that at least some activity of the *mth* gene is essential for survival. When mutated, the intermediate level of expression of a hypomorphic allele might adjust response to stress in a way that is more favorable for survival, whereas full expression of the normal gene exceeds the optimum value. The delicate balance among the embryonic lethality of a null allele, enhanced longevity of a hypomorphic allele, and the normal wild phenotype suggests that the level of *mth* gene expression is an important component of the system controlling life-span. Investigation of the gene's function and associated pathways should lead to better understanding of mechanisms relevant to aging.

References and Notes

1. M. R. Rose and B. Charlesworth, *Nature* **287**, 141 (1980); *Genetics* **97**, 173 (1981); *ibid.*, p. 187.
2. D. B. Friedman and T. E. Johnson, *Genetics* **118**, 75 (1988); S. Hekimi, P. Boutis, B. Lakowski, *ibid.* **141**, 1351 (1995); C. Kenyon *et al.*, *Nature* **366**, 461 (1993).
3. J. Z. Morris, H. A. Tissenbaum, G. Ruvkun, *Nature* **382**, 536 (1996); J. J. Ewbank *et al.*, *Science* **275**, 980 (1997); S. Hekimi *et al.*, *Trends Genet.* **14**, 14 (1998).
4. K. D. Kimura *et al.*, *Science* **277**, 942 (1997).

5. G. J. Lithgow *et al.*, *J. Gerontol.* **49**, B270 (1994); G. J. Lithgow *et al.*, *Proc. Natl. Acad. Sci. U.S.A.* **92**, 7540 (1995).
6. P. L. Larsen, *Proc. Natl. Acad. Sci. U.S.A.* **90**, 8905 (1993); J. R. Vanfleteren, *Biochem. J.* **292**, 605 (1993).
7. P. M. Service *et al.*, Physiol. Zool. **58**, 380 (1985).
8. J. L. Graves *et al.*, *ibid.* **65**, 268 (1992).
9. R. Arking *et al.*, *Dev. Genet.* **12**, 362 (1991).
10. W. C. Orr and R. S. Sohal, *Science* **263**, 1128 (1994).
11. T. Parkes *et al.*, *Nature Genet.* **19**, 171 (1998).
12. L. Cooley, R. Kelley, A. Spradling, *Science* **239**, 1121 (1988).
13. To generate P-element insertion lines, we crossed females carrying eight copies of P{*lac*W} (*25*) on a compound X chromosome (C(1)RM) with *ry Ki* P{ry^+ Δ2-3}, which carries the transposase. Female progeny were then crossed individually with w^{1118}. New P-element insertions on autosomes were identified by red eye color in male progeny. In any cross that generated progeny having different degrees of red eye color, suggestive of multiple insertions, we chose a single female with lighter eye color and back-crossed it to w^{1118} for several generations, until the color was homogeneous. Each insertion was mapped to a chromosome by the use of balancers, tested for homozygous viability and fertility, and established as an independent line. After its isolation, *mth* was extensively out-crossed before further characterization to avoid nonspecific effects of genetic background (*26*).
14. F. M. Ashton and A. S. Crafts, *Mode of Action of Insecticide* (Wiley Interscience, New York, 1973).
15. A. R. Heydari *et al.*, *Experientia* **50**, 1092 (1994); J. C. Wheeler, E. T. Bieschke, J. Tower, *Proc. Natl. Acad. Sci. U.S.A.* **92**, 10408 (1995).
16. M. Tatar, A. A. Khazaeli, J. W. Curtsinger, *Nature* **390**, 30 (1997).
17. The *mth* genomic DNA was probed by the ampicillin resistance gene contained in the P-element construct used to generate mutant lines (*25*).
18. To excise the P-element, we crossed *mth* females with *ry Ki* P{ry^+ Δ2-3}. The male jump-starters were then crossed to *w*;TM3/TM6. Progeny with white eyes were made homozygous and lines established. Two alleles were homozygous lethal before the L2 larval stage and so were maintained over the third chromosome balancers, TM3 or TM6.
19. Genomic DNA adjacent to the P-element insertion site in *mth* was retrieved by plasmid rescue (*27*). Pst I and Eco RI digestion were used to clone upstream and downstream genomic fragments (Fig. 3A). Analysis of the upstream DNA sequence by Blast search (*28*) revealed two homologous sequences (clones LD08316 and GM02553) in the Berkeley *Drosophila* Genome Project (BDGP) database. The GM02553 clone, despite containing regions with 67% identity to the *mth* nucleotide sequence, had 17 gaps in the alignment, so it is not the same gene. In contrast, the 747-nucleotide partial sequence of LD08316 in the BDGP database displayed greater than 99% identity to the upstream sequence, without any gap. The calculated smallest sum probability of the Blast search was 1.5×10^{-137}, well within the range of identical sequences. The full sequence of LD08316 (1948 nucleotides) (Fig. 3B) also corresponded to the downstream genomic sequence of *mth*. We then used the cDNA as a probe to isolate *mth* genomic DNA from a P1-phagemid grid from Genome Systems. Three P1 plasmids (DS05332, DS03799, and DS06692) from the BDPG contained the genomic region of the *mth* gene. These P1 clones have a common contig, DS00539, which maps at 61C on the third chromosome (BDGP database). A corresponding 7.9-kb Eco RI fragment from DS06692 was subcloned into pBluescript vector and the full-length sequence determined.
20. S. F. Altschul *et al.*, *Nucleic Acids Res.* **25**, 3389 (1997).
21. S. Henikoff and J. G. Henikoff, *Genomics* **19**, 97 (1994).
22. B. K. Kobilka *et al.*, *Science* **240**, 1310 (1988); T. Kubo *et al.*, *FEBS Lett.* **241**, 119 (1988); S. K. Wong, C. Slaughter, A. E. Ruoho, E. M. Ross, *J. Biol. Chem.* **263**, 7925 (1988); J. Ostrowski, M. A. Kjelsberg, M. G. Caron, R. J. Lefkowitz, *Annu. Rev. Pharmacol. Toxicol.* **32**, 167 (1992); E. S. Burstein, T. A. Spalding, M. R. Brann, *Biochemistry* **37**, 4052 (1998).
23. G. A. Walker, D. W. Walker, G. J. Lithgow, *Ann. N.Y. Acad. Sci.* **851**, 444 (1998).
24. S. Watson and S. Arkinstall, *The G-protein Linked Receptor Facts Book* (Academic Press, London, 1994); G. Vassart *et al.*, *Ann. N.Y. Acad. Sci.* **766**, 23 (1995); T. P. Sakmar, *Prog. Nucleic Acid Res. Mol. Biol.* **59**, 1 (1998).
25. E. Bier *et al.*, *Genes Dev.* **3**, 1273 (1989).
26. J. Tower, *Bioessays* **18**, 799 (1996).
27. B. A. Hamilton and K. Zinn, in *Methods in Cell Biology*, L. S. B. Goldstein and E. A. Fryberg, Eds. (Academic Press, San Diego, 1994), vol. 44, p. 81.
28. S. F. Altschul *et al.*, *J. Mol. Biol.* **215**, 403 (1990).
29. J. Kyte and R. F. Doolittle, *ibid.* **157**, 105 (1982).
30. Supported by a Postdoctoral Research Fellowship from the John Douglas French Alzheimer Foundation (Y.-J.L.) and grants from the National Science Foundation (MCB9408718), the National Institutes of Health (EY09278 and AG12289), and the James G. Boswell Foundation (S.B.).

14 July 1998; accepted 25 September 1998

Cardiovascular Failure in Mouse Embryos Deficient in VEGF Receptor-3

Daniel J. Dumont,*† Lotta Jussila,* Jussi Taipale,* Athina Lymboussaki, Tuija Mustonen, Katri Pajusola, Martin Breitman,‡ Kari Alitalo§

Vascular endothelial growth factor (VEGF) is a key regulator of blood vessel development in embryos and angiogenesis in adult tissues. Unlike VEGF, the related VEGF-C stimulates the growth of lymphatic vessels through its specific lymphatic endothelial receptor VEGFR-3. Here it is shown that targeted inactivation of the gene encoding VEGFR-3 resulted in defective blood vessel development in early mouse embryos. Vasculogenesis and angiogenesis occurred, but large vessels became abnormally organized with defective lumens, leading to fluid accumulation in the pericardial cavity and cardiovascular failure at embryonic day 9.5. Thus, VEGFR-3 has an essential role in the development of the embryonic cardiovascular system before the emergence of the lymphatic vessels.

Disruption of VEGF or either of its two receptors VEGFR-1 (Flt-1) or VEGFR-2 (Flk-1) results in early embryonic death because of a failure of blood vessel development (*1–4*). The related placenta growth factor (PlGF) and VEGF-B signal through VEGFR-1 (*5*), whereas VEGF-C and VEGF-D can use both VEGFR-3 and VEGFR-2 for signaling (*6–8*). The expression of VEGFR-3 (Flt4) starts during mouse embryonic day (E) 8 in developing blood vessels but becomes largely restricted to the lymphatic vessels after their formation (*9*).

To analyze the biological role of VEGFR-3, we generated mice lacking a functional gene encoding VEGFR-3 by a knock-in strategy in which the bacterial β-galactosidase gene (*LacZ*) was placed in the first coding exon under the control of the transcriptional regulatory sequences of VEGFR-3, deleting the beginning of the protein-coding region (Fig. 1) (*10*). The β-galactosidase (β-Gal) marker allows analysis of the pattern of VEGFR-3 gene expression in the gene-targeted mice.

Heterozygous mice and embryos appeared phenotypically normal, and the β-Gal expression in their tissues was consistent with that observed in VEGFR-3 in situ hybridization analysis of tissue sections (*9*). For example, large pericardial lymphatic vessels were detected in whole-mount staining of the heart of a newborn VEGFR-$3^{+/-}$ mouse (Fig. 2A), whereas only blood vessels were stained in a similar analysis of Tie-$1^{+/-}$ mice (*11*), which express β-Gal in endothelial cells (*12*). The stained vessels did not contain erythrocytes in sections of newborn skin, confirming their lymphatic nature (Fig. 2B). Also in E14.5 embryos, the developing lymphatic network of the skin was strongly stained, for example, around the developing ear (Fig. 2C). At E13.0, the expression was most prominent in venous sacs in the jugular and mesonephric regions and their surrounding vessels, supporting Sabin's theory on the origin of the first lymphatic vessels (*13*) (Fig. 2D).

To date, no live-born VEGFR-$3^{-/-}$ mice have been found. To determine the onset of embryonic lethality, we isolated embryos at

D. J. Dumont, Ontario Cancer Institute and Amgen Institute, Department of Medical Biophysics, University of Toronto, Toronto, Ontario, Canada M5G 2C1. L. Jussila, J. Taipale, A. Lymboussaki, T. Mustonen, K. Pajusola, K. Alitalo, Molecular/Cancer Biology Laboratory, Haartman Institute, University of Helsinki, PL 21 (Haartmaninkatu 3), 00014 Helsinki, Finland. M. Breitman, Samuel Lunenfeld Research Institute, Mount Sinai Hospital, Toronto, Ontario M5G 1X5, Canada.

*These authors contributed equally to this work.
†Present address: Sunnybrook Health Science Centre, Division of Cancer Biology, S Wing Research Building, 2075 Bayview Avenue, Toronto, Ontario, M4N 3M5, Canada. ‡Deceased. §To whom correspondence should be addressed. E-mail: Kari.Alitalo@Helsinki.FI